AGU ADVANCING EARTH AND SPACE SCIENCE

Water Resources Research

RESEARCH ARTICLE
10.1029/2020WR028693

Prediction of Hypoxia in Eutrophic Polymictic Lakes

A. Cortés[1,2], A. L. Forrest[1,2], S. Sadro[1,3], A. J. Stang[1,2], M. Swann[1,2], N. T. Framsted[1,3], R. Thirkill[1,2], S. L. Sharp[1,2], and S. G. Schladow[1,2]

[1]Tahoe Environmental Research Center, University of California Davis, Davis, California, USA, [2]Department of Civil and Environmental Engineering, University of California Davis, Davis, California, USA, [3]Department of Environmental Science and Policy, University of California Davis, Davis, California, USA

Key Points:

- We present a new one-dimensional method to estimate onset and duration of hypoxic events in eutrophic polymictic lakes
- The model only requires basic meteorological variables, lake surface temperatures, and dissolved oxygen at the lake bottom for calibration
- The method can be a cost-effective decision-making tool for management actions affecting ecosystem health and water quality

Supporting Information:

Supporting Information may be found in the online version of this article.

Correspondence to:

A. Cortés,
alicortes@ucdavis.edu

Citation:

Cortés, A., Forrest, A. L., Sadro, S., Stang, A. J., Swann, M., Framsted, N. T., et al. (2021). Prediction of hypoxia in eutrophic polymictic lakes. *Water Resources Research*, *57*, e2020WR028693. https://doi.org/10.1029/2020WR028693

Received 26 AUG 2020
Accepted 11 MAY 2021

Abstract Quantifying and predicting the drawdown of dissolved oxygen (DO) in lakes is important to ensuring healthy ecosystems and safe water sources. The characterization of DO depletion using available definitions and models requires extensive monitoring to obtain reliable results. These approaches have been mostly developed for seasonally stratified monomictic and dimictic lakes, limiting their applicability for polymictic systems which stratify and mix repeatedly. We compared the predicted duration of hypoxic events in the three basins of a large eutrophic polymictic lake (Clear Lake, CA, USA) by using three different one-dimensional (1-D) analytical approaches; two being original and requiring minimal input variables. Data on meteorology, lake temperature, and DO were all measured at multiple locations for one year and used to develop a novel method, named the *Birge-Winkler* method. The daily net surface heat fluxes provided an energy term from which estimates of the onset and length of hypoxic periods could be made with minimal calibration. We used the *Lake Number* method to evaluate the level of accuracy of the *Birge-Winkler* method. Finally, we estimated DO values next to the sediments using a *Buoyancy Frequency* method. Our results from the two original methods provided simple and effective tools for early warning of onset and duration of hypoxia, with a maximum of ±3–5 days uncertainty in the predictions. These indices can become powerful decision support tools for addressing aquatic ecological challenges triggered by hypoxia, including fish kills, internal nutrient loading, heavy metals release, and harmful algal blooms.

1. Introduction

Dissolved oxygen (DO) is essential for maintaining healthy aquatic ecosystems, thus, the depletion of DO in lakes remains an important research topic (Kalff, 2002). DO depletion can have significant implications across trophic levels, from increasing harmful algal blooms (HABs) to reducing fish habitat (Diaz & Rosenberg, 2008). The main sinks of DO in aquatic ecosystems include biological and biogeochemical processes occurring in both the water column and at the sediment–water interface (Bouffard et al., 2013; Müller et al., 2012). Hypoxia in lakes and reservoirs has increased over the past century mainly as a result of an increased demand for DO stemming from excessive nutrient loading or eutrophication (Schindler et al., 2016). Ongoing changes in climate are expected to increase hypoxia in many lakes by stimulating rates of respiration more than primary production, and by increasing thermal stratification and reducing the frequency of mixing events (Adrian et al., 2009; Yvon-Durocher et al., 2010). Regardless of the mechanism, extended periods of hypoxia can alter redox potential and lead to internal loading of nutrients from sediments (Welch & Cooke, 1995), further contributing to eutrophication, HABs, and deteriorated water quality. Thus, simple and cost-efficient ways of quantifying and predicting the drawdown of DO in lakes and reservoirs is a priority for limnologists and water managers to ensure ecosystem health and maintain water quality standards.

A wide variety of tools have been developed to make direct measurements of DO in aquatic ecosystems, ranging from the traditional Winkler titration to optical oxygen sensors. Limnologists have utilized various approaches for quantifying DO depletion rates. These include the areal hypolimnetic oxygen demand (AHOD, g DO m^{-2} d^{-1}), which quantifies DO depletion rates down to 2 mg L^{-1}, and the anoxic/hypoxic factor (AF/HF, d $season^{-1}$) which estimates the number of days that an area equal to the lake bottom is exposed to anoxia/hypoxia, a proxy of the length of time that anoxia/hypoxia persists (Nürnberg, 2002). More recently, Matzinger et al. (2010) developed the concept of aerial hypolimnetic mineralization rates (AHM, g DO m^{-2} d^{-1}) to include the fluxes of reduced substances (e.g., methane and ammonium) released from the sediments under anoxic conditions. Other current studies have successfully tested the relationship between

Table 1
List of Polymictic Eutrophic Lakes and Reservoirs Around the World and Their Characteristics

Name	Country	Maximum depth, z_{max} (m)	Surface area, S_A (km^2)	Reference
Lake Taihu	China	3	2,338	Qin et al. (2010)
Saskatoon Lake	Canada, Alberta	4	7.5	Taranu et al. (2010)
Lake Wingra	USA, WI	4	1.4	Magee and Wu (2017)
Cooking Lake	Canada, Alberta	4.6	36	Taranu et al. (2010)
Lake Müggelsee	Germany	8	7.3	Wilhelm and Adrian (2008)
Lake Elsinore	USA, CA	13	14.6	Martinez and Anderson (2013)
Upper Arm (Clear Lake)	USA, CA	11	106	This study
Oaks Arm (Clear Lake)	USA, CA	14	15	This study
Lower Arm (Clear Lake)	USA, CA	15	30	This study
Kranji Reservoir	Singapore	17	3	Yang et al. (2015)

oxygen depletion and the hypolimnetic depth (Müller et al., 2012) or the phosphorus flux supply (Müller et al., 2019). However, all of these approaches require substantial in situ measurements of DO, and none of them predict the onset of hypoxia.

Numerical models represent a powerful tool to predict the long-term DO dynamics in aquatic ecosystems. Changes in DO are simulated using process-based biogeochemical models that parameterize photosynthesis, reaeration, respiration, biochemical oxygen demand, and sediment oxygen demand. The distribution of DO in the domain change due to physical processes (mixing, stratification, transport), and biogeochemical processes. This exists for both 1-D (Rucinski et al., 2010; Schladow & Hamilton, 1997) and 3-D models (Leon et al., 2011; Peña et al., 2010). Both modeling approaches require significant data during the calibration and validation process for a specific site.

Simpler analytical models that require fewer or more easily measured input variables and minimal calibration can be of significant value. Walker (1979) tested empirical models to relate the trophic state of the lake with the hypolimnetic oxygen depletion rate. Robertson and Imberger (1994) developed a simple model that related changes in Lake Number (L_N), or the extent of mixing, to changes in the near-bottom DO concentrations. Given the importance of stratification on DO depletion, lake mixing dynamics modeled using meteorological drivers, such as the well-established net surface heat flux approach (Imberger, 1985; MacIntyre et al., 2002), is also of considerable value. Computing the extent of mixing from basic meteorology and linking that to oxygen depletion may provide one of the simplest and most cost-effective tools to predict hypoxia in aquatic ecosystems.

However, most definitions and predictive tools for understanding DO depletion extend from knowledge of deep, monomictic and dimictic lakes (Müller et al., 2012, Table 1). Shallow polymictic lakes are still poorly understood and only a few studies about hypoxia have focused on them (Taranu et al., 2010). Polymictic lakes are highly dynamic (Table 1); subtle changes in meteorological forcing can stratify or mix these shallow water bodies multiple times a year (Rueda, Schladow, et al., 2003; Wilhelm & Adrian, 2008). Their large fraction of water exposed to sediments make them particularly vulnerable to internal nutrient loading associated with periods of anoxia/hypoxia. The excessive nutrient input may exacerbate eutrophication and occurrence of HABs (Orihel et al., 2017). Consequently, simple ways of predicting the onset of hypoxia in polymictic lakes have value both as a warning tool, which might trigger mitigation actions such as oxygenation, and as means of estimating sediment release rates.

In this study, we compare predictions for the onset and duration of hypoxic events in each basin of a eutrophic, multibasin polymictic lake (Clear Lake, CA, USA) using three different 1-D analytical models. Two of these models are novel and we show that they are accurate using readily acquired input variables. Our methods provide a quick and cost-effective tool for early warning of the onset and duration of hypoxia.

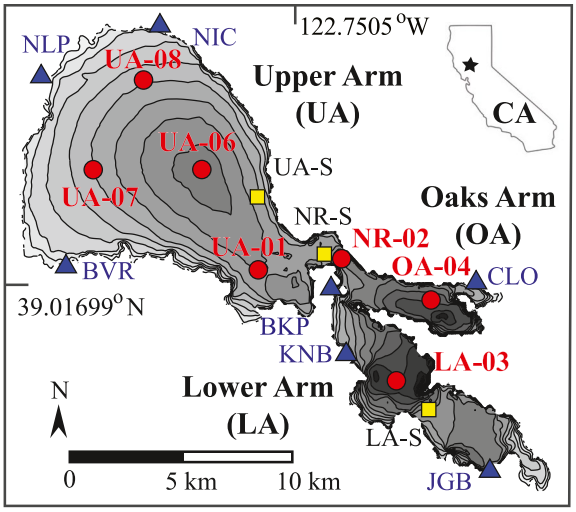

Figure 1. Bathymetry of Clear Lake, CA with contours every 2 m. Red circles mark the location of seven continuously measuring moorings and profiling sites. Blue triangles are the meteorological stations and surface inshore temperature loggers. Yellow squares mark the three near-surface offshore thermistor chains.

2. Study Site

Clear Lake, (39°00′N, 122°45′W), located in the Coastal Range of Northern California, USA, is a large, shallow lake with a surface area (S_A) of 151 km^2, mean depth of 8 m, and maximum depth (Z_{max}) of ~15 m, depending on the lake water level (maximum annual changes in water surface elevation ~3 m). The system tends to mix several times annually, is naturally eutrophic, and has a multibasin bathymetry (Text S1). Three different sub-basins exist: Upper Arm, Lower Arm, and Oaks Arm (Figure 1, Table 2). The Upper Arm (UA) is the largest and shallowest basin, and directly receives >90% of the watershed runoff. A passage at the east end of the UA referred to as the Narrows (NR) connects it with two smaller and deeper basins. The Lower Arm (LA) connects to the only outlet at the southeast end of the lake, while the Oaks Arm (OA) is the smallest basin and extends east of the Narrows. The residence time of the lake is about 4.5 years (Richerson, Suchanek, & Why, 1994). The wind field and stratification, modulated by the Earth's rotation, are the main drivers of transport within individual basins and between them (Rueda et al., 2003, 2008). Given the long residence time (years) and the polymictic nature of all the basins (vertically mixes and re-stratifies multiple times each summer), the impact of advection between basins on the vertical dynamics is considered minor, and a one-dimensional (vertical) approach is considered adequate for what follows.

3. Field Methods

3.1. Meteorology

Meteorological data were obtained from seven stations installed on docks on the shoreline of Clear Lake (Figure 1). Here, we present data for the year spanning March 2019 to February 2020. Those stations are Nice (NIC), North Lakeport (NLP), Big Valley Rancheria, (BVR), Konocti Bay (KNB), Jago Bay (JGB), Buckingham Point (BKP), and Clearlake Oaks (CLO). BVR was ~200 m inland from the shoreline. Air temperature, relative humidity, incoming shortwave solar radiation, precipitation, wind speed and direction were measured every 15 min with Davis Instruments Wireless Vantage Pro2 Plus meteorological stations. At each site (except BVR), we also deployed water temperature sensors (Onset Water Temp Pros with 0.2°C accuracy, 0.02°C resolution) ~0.5 m below the lake surface sampling every 10 min.

3.2. Moored Instrumentation

Time-series measurements of lake temperature and DO were recorded at seven moorings (Figure 1). We deployed taut-line moorings with a subsurface buoy 2–3 m below the surface starting in March 2019 and

Table 2
Inshore and Offshore Shallow Loggers Used in the Linear Regressions to Estimate Long-Term Offshore Surface Temperatures From Surface Inshore Time Series, and the Subsurface Mooring Associated to Each Lake Surface Time Series

Inshore logger	Offshore logger	Linear regression coefficients	R^2	Subsurface Mooring	Meteorological station
KNB	LA-S	[0.99, −0.78]	0.98	LA-03	KNB
BKP	NR-S	[1.03, −0.76]	0.91	NR-02, UA-01	BKP
CLO	NR-S	[0.99, −0.80]	0.93	OA-04	BKP
NLP	UA-S	[1.01, −0.95]	0.87	UA-07, UA-8	NLP
NIC	UA-S	[1.01, −0.72]	0.95	UA-06	NIC

Note. The meteorological station upwind of the predominant wind direction for each arm is also listed.

here present data for the year spanning March 2019 to February 2020. Instruments were serviced every 3–4 months. Each subsurface mooring had a set of RBR solo^{3}T thermistors (0.002 °C accuracy, 0.0002 °C resolution) spaced ~1 m throughout the water column recording water temperatures every 10 s. Moorings had one to three wiped DO sensors which measured every 30 s or 10 min, depending on their manufacturer. RBR codaT.ODO dissolved oxygen sensors or RBR-DO (accuracy 0.26 mg L^{-1}, and resolution <0.03 mg L^{-1}) sampled faster than the PME miniDOT dissolved oxygen sensors (accuracy 0.3 mg L^{-1}, and resolution of 0.01 mg L^{-1}). The three deepest moorings at each basin (LA-03, OA-04, UA-06) had two near-sediment RBR-DO sensors 0.5 and 2 m off the bottom with a miniDOT sensor in the epilimnion ~4–5 m below the surface. Other moorings had only one RBR-DO sensor 0.5 m off the bottom. An Onset HOBO U20-001-01 water depth sensor (accuracy 0.5 cm, and resolution of 0.21 cm) on each mooring line sampling hourly allowed for the determination of the depth of each logger and the changing lake water level during the study period. Lake level was also monitored with a pressure transducer installed at Lakeport by the United States Geological Survey's (USGS) National Water Information System (NWIS) (https://waterdata.usgs.gov/ca/nwis/uv?site_no=11450000).

3.3. Lake Surface Temperatures

We used modified lake temperature time series from the inshore loggers adjacent to the meteorological stations to fill the near-surface lake temperature gap from the subsurface moorings. Due to the shallowness of the lake next to the docks, inshore near-surface temperatures normally exceeded the surface offshore temperatures. We measured near-surface offshore temperatures using arrays of thermistors installed in the upper 2 m of the lake water column attached to navigation markers at three locations across the lake (Figure 1, UA-S, NR-S, LA-S). Each shallow offshore array was housed inside a perforated PVC pipe suspended from a buoy. Onset Water Temp Pros sensors were located every 0.5 m. These shallow offshore thermistor chains only provided reliable data during short periods throughout our year of sampling. Therefore, we developed linear regression equations with the near-surface offshore being dependent on inshore temperatures. We used the closest shallow offshore array to regress each surface inshore time series (Table 2). On average, offshore lake surface temperatures were 0.72–0.95 °C colder than the inshore values (minimum $R^2 = 0.87$). This correlation also held when temperatures offshore were measured with a temperature profiler in the middle of each basin. We assumed linear temperature changes in depth between the modified surface lake temperature time series from the inshore loggers and the shallowest subsurface logger of the taut-line moorings.

3.4. Profiling Data

Profiles of physico-biogeochemical properties of the lake water adjacent to the seven moorings were collected every ~6 weeks using a Seabird SBE-19plus water quality profiler. Electrical conductivity, temperature, depth, chlorophyll-*a*, turbidity, and DO were measured. Temperature and DO time series from the mooring stations were intercalibrated against these profiles. We measured lake clarity using a Secchi disk, and photosynthetically active radiation (PAR) throughout the water column using a LiCOR L1400 profiler (Table S1).

4. Analytical Methods

We predicted the onset and duration of hypoxia using three different one-dimensional (1-D) methods: *Birge-Winkler* (BIW), *Lake Number* (L_N), and *Buoyancy Frequency* (N). This section describes the analytical approach for each method. We quantified their accuracy by comparing the modeled and measured length of hypoxia via two performance metrics: the root mean square error computed as RMSE = $\left(\sum\left(x_{mod} - x_{mes}\right)^2 / N_x\right)^{0.5}$, and the Nash-Sutcliffe model efficiency coefficient estimated as NSE = $1 - \left[\sum\left(x_{mod} - x_{mes}\right)^2 / \sum\left(x_{mes} - \overline{x_{mes}}\right)^2\right]$, where x_{mod} and x_{mes} are modeled and measured data points, respectively, $\overline{x_{mes}}$ is the mean value across all measured data points, and N_x the number of measured data

points. Model performance characterized by the NSE can be excellent (0.65–1), very good (0.5–0.65), good (0.2–0.5), poor (0–0.2), and very poor (<0) (Allen et al., 2007).

4.1. Birge-Winkler Method

We named this the *Birge-Winkler* (BIW) method, after the pioneering work on heat budgets and dissolved oxygen measurements by E. A. Birge and L. W. Winkler, respectively (Kalff, 2002). A daily net surface heat flux (NSHF) is used to estimate the onset of hypoxic events; thus, only meteorological forcing is considered to affect the onset and duration of hypoxia. This is a reasonable assumption for polymictic waterbodies since lake stratification changes quickly and meteorological forcing is the main driver.

4.1.1. Net Surface Heat Flux (NSHF)

The lake surface energy budget was calculated using bulk mass-transfer coefficients adjusted for atmospheric stability following Imberger (1985) and MacIntyre et al. (2002). The NSHF (W m^{-2}) was computed as the sum of the net shortwave radiation (SW_{net}), net longwave radiation (LW_{net}), sensible heat flux (SE) and latent heat flux (LE). Net values of shortwave and longwave radiation were obtained by subtracting the outgoing from the incoming fraction ($SW_{net} = SW_{in}–SW_{out}$; $LW_{net} = LW_{in}$ - LW_{out}). SW_{out} was calculated as a fraction of SW_{in}, using the albedo (α) of the lake surface ($SW_{out} = \alpha\ SW_{in}$). Albedo was estimated taking into account the zenith angle and the angle of refraction (Neumann & Pierson, 1966). LW_{in} was calculated as a function of the air temperature, T_a (°C), and cloud cover, *cc* (Martin & McCutcheon, 1999) as, $LW_{in} = 0.909 \times 10^{-5} \times (1 + 0.17 \times cc) \times 5.67 \times 10^{-8} \times [(T_a + 273.16)^6]$, where *cc* is the ratio between the measured SW_{in} and the theoretical SW_{in}. We estimated the theoretical SW_{in} taking into account the latitude, declination of the sun, date, and hour angles (Martin & McCutcheon, 1999). LW_{out} was computed from the lake surface temperature using the Stefan-Boltzmann equation (MacIntyre et al., 2002). SE and LE were estimated given the equations,

$$SE = \rho_a\ C_{pa}\ c_m\ U\left(T_s - T_a\right) \tag{1}$$

$$LE = \rho_a\ L_v\ c_m\ U\left(q_s - q_a\right) \tag{2}$$

where ρ_a is the air density (= 1.2 kg m^{-3}), C_{pa} is the specific heat of air (= 1,004 J kg^{-1} °C^{-1}), c_m is the corrected mass-transfer coefficient, L_v is the latent heat of vaporization (= 2.5×10^6 J kg^{-1}), U is wind speed (m s^{-1}), T_s and T_a are water surface and air temperature (°C), respectively, q_s is the specific humidity at saturation at T_s, and q_a is the specific humidity of the air (mbar). We corrected the neutral value of the mass transfer coefficient to take into account the atmospheric stability using the iterative approach described by Hicks (1975) following MacIntyre et al. (2002). Heat advection due to stream inflows and outflows, groundwater, and rain were all assumed negligible.

4.1.2. Prediction of Hypoxia Using the Birge-Winkler (BIW) Method

We used the BIW method to estimate the onset and duration of hypoxia in Clear Lake. Each basin was considered to be an independent water body (Table 1) as the interbasin exchange flows relative to their volumes were assumed to be small. We used the regressed surface lake temperature measured at the deepest mooring at each basin (LA-03, OA-04, UA-06) and the meteorological station upwind of the predominant wind direction for each arm (Table 2). Daily values of the surface heat fluxes for each basin (SW_{net}, LW_{net}, SE, LE) were computed as the sum of the hourly values in one day (W m^{-2}) multiplied by the interval of time, *dt* (3600 s). Thus, daily time series of NSHF (J m^{-2}) were obtained by adding the different daily surface heat flux terms.

We subsequently calculated the time series of cumulative daily NSHF divided by the maximum depth (z_{max}) of the basin (J m^{-3}) for a specific number of days (t_n). This energy per unit volume term, BIW, is computed as,

$$BIW\left[\mathrm{J\ m^{-3}}\right] = \sum_{t=1}^{t_n} \frac{NSHF\left[\mathrm{J\ m^{-2}}\right]}{z_{max}\left[\mathrm{m}\right]} \tag{3}$$

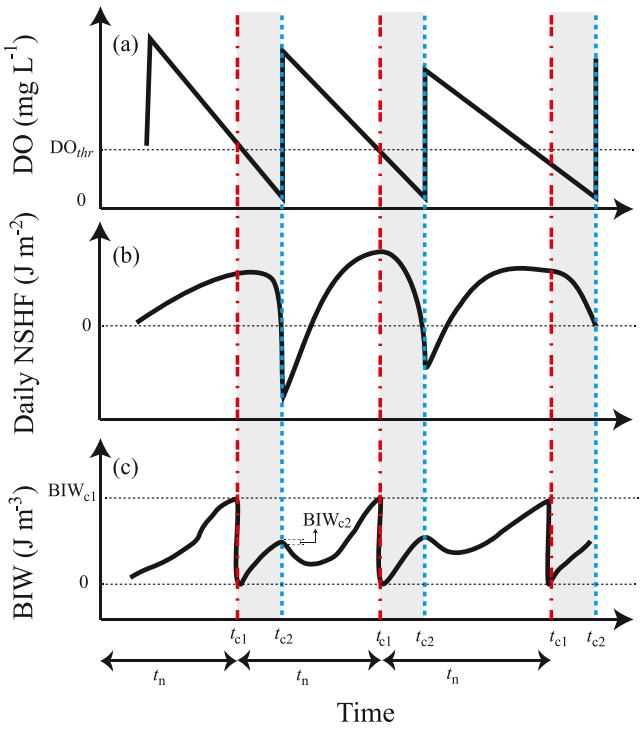

Figure 2. Diagram describing the BIW method. (a) Hypothetical DO concentrations at the sediment–water interface, (b) daily NSHF time series, (c) BIW energy term computed using (b) and Equation 3 when DO drops below a certain threshold (DO_{thr}) at the onset of hypoxia on day t_{c1} which yields a critical energy value BIW_{c1} (red dashed-dotted line). The blue dashed line marks the end of the hypoxic period (t_{c2}) when DO values experience a sudden increase and the daily rate of change for BIW is smaller than -10^5 J m^{-3} (BIW_{c2}). The gray rectangles mark the length of the hypoxic period, and t_n is the number of days between the onset of two consecutive hypoxic events.

where the number of days between the onset of two consecutive hypoxic events, t_n, was defined by selecting the dates t_{c1} when DO levels at the sediment–water interface dropped below a threshold, DO_{thr} (Figure 2). As a result, we defined the cumulative energy BIW value to characterize the beginning of the hypoxic period on day t_{c1}, named BIW_{c1}. After we reached the cut-off value BIW_{c1}, we initiated the summation using Equation 3 for t_n days until the onset of the next hypoxic event on the next t_{c1}. The BIW_{c1} was a calibration parameter of our model for each basin. This cut-off value also changed depending on the DO_{thr} used to define hypoxia, as discussed in detail below.

The *Birge-Winkler* method provides an estimate of the length of hypoxic events by determining the beginning and end of such periods. The beginning of the hypoxic period on day t_{c1} is when the energy term BIW = BIW_{c1}. The end of the hypoxic period occurs when the BIW energy term experiences a sudden drop in 24 h, such that the rate of change in BIW between two consecutive days was smaller than -10^5 J m^{-3}, named BIW_{c2} (Figure 2c). BIW_{c2} was found to have always the same value for all basins and DO_{thr}, as opposed to BIW_{c1}. As a result, we were able to define the length of the hypoxic period as the difference between end and start dates ($t_{c2} - t_{c1}$). We validated our estimates of the length of the hypoxic period using the time series of measured DO concentrations taken at the sediment–water interface.

We calibrated the cumulative energy BIW value to characterize the beginning of the hypoxic period, BIW_{c1}, for each basin and DO_{thr} (Table 3). For example, mild and severe hypoxia and avoidance for fish have been defined when DO values are lower than 4 mg L^{-1} and 2 mg L^{-1}, respectively (Biddanda et al., 2018; Feyrer et al., 2020). The fish tolerance to hypoxia also changes with fish species. In Clear Lake, native species seem to be more sensitive to low levels of DO (e.g., Clear Lake hitch, prickly sculpin, tule perch) than non-native species (e.g., white catfish, carp, largemouth bass, bluegill, goldfish) (Thompson et al., 2013). Hypoxia at the sediment–water interface can also trigger internal loading. Nürnberg et al. (2013) used a DO_{thr} of ~3 mg L^{-1} under which they expected internal loading to occur. Laboratory experiments for Clear Lake sediments by the authors show that the release of nutrients started when DO was below 1 mg L^{-1} (unpublished data). As a result, we presented graphical results of the *Birge-Winkler* method assuming a DO_{thr} of 3 mg L^{-1}, which yielded a BIW_{c1} value ranging between 1.6×10^7 and 2.4×10^7 J m^{-3} for the three basins of Clear Lake (mean ~2×10^7 J m^{-3}). Then, we performed a sensitivity analysis of the BIW_{c1} value for DO_{thr} ranging between 1 and 4 mg L^{-1} (Table 3).

Table 3
Values at the Onset of Hypoxia of the Energy Term BIW_{c1} (J m^{-3}), for Different DO_{thr} Values, and Three Basins in Clear Lake

DO threshold	1 mg L^{-1}	2 mg L^{-1}	3 mg L^{-1}	4 mg L^{-1}
Basin	Threshold for internal loading	Threshold for fish avoidance	Threshold for both internal loading and fish avoidance	Maximum threshold for fish avoidance
Lower Arm	1.91×10^7	1.87×10^7	1.81×10^7	1.76×10^7
Oaks Arm	1.71×10^7	1.66×10^7	1.61×10^7	1.55×10^7
Lower Arm	2.52×10^7	2.45×10^7	2.38×10^7	2.31×10^7

4.2. Lake Number (L_N) Method

The Lake Number (L_N) describes the ratio between stratifying and mixing forces, which can impact water quality such as dissolved oxygen (Robertson & Imberger, 1994). Calculation of L_N requires lake temperature, wind, and hypsographic data and is defined as,

$$L_N = \frac{g\, S_t \left(1 - z_t / z_{max}\right)}{\rho_0\, u_*^2\, A_0^{3/2} \left(1 - z_g / z_{max}\right)} \quad (4)$$

$$S_t = \int_z^{z_{max}} \left(z - z_g\right) A(z)\, \rho(z)\, dz \quad (5)$$

where g is the acceleration of gravity (= 9.8 m s^{-2}), z_t is the thermocline height, z_g is the center of volume above the bottom, ρ is water density at the surface or different depths (z) computed only from temperature following Chen and Millero (1986) since salinity contribution was negligible, A is lake surface area, u_* is water friction velocity, and S_t is the Schmidt Stability. Assuming that the shear stress at the air–water interface is the same on both sides, we computed u_* on the water side as $\left[\left(\rho_a/\rho_w\, C_D\right)^{0.5} U\right]$, where ρ_a and ρ_w are the air and water densities, respectively, C_D is the momentum transfer coefficient (=1.3 × 10^{-3}), and U is the magnitude of the wind. This 1-D model requires a larger amount of input data than the previous *Birge-Winkler* method. We used the L_N approach to evaluate the performance of the BIW method since it considers both the changes in the lake stratification and the meteorological forcing.

When $L_N < 1$, wind shear overcomes the stratification and deep mixing can occur, while if $L_N > 1$ the strength of the stratification suppresses mixing. If mixing is suppressed, DO depleted hypolimnetic waters can develop due to the lack of exchange with the atmosphere. Thus, Robertson and Imberger (1994) used daily L_N values to estimate changes in the near-sediment DO concentrations assuming two main phases:

- Phase 1 was characterized by $L_N > 1$, and DO values were mainly depleted due to bio-chemical consumption (a, %), and computed as,

$$DO_b(t) = DO_b(t-1) - a\,\Delta t \tag{6}$$

- In Phase 2, the isolation ended, $L_N < 1$, and DO values increased as a result of mixing between deep and surface layers that authors quantified using the following equation,

$$DO_b(t) = DO_b(t-1) + \frac{K_z\left[DO_s(t-1) - DO_b(t-1)\right]\Delta t}{H^2} \tag{7}$$

where DO is expressed as a percentage of DO saturation (%) at the surface (s) and the bottom (b) of the system, a (%) is the rate of DO consumption next to the sediments, K_z (m^2 s^{-1}) is the depth average eddy diffusivity in the water column, Δt (s) is the time increment between t and (t-1), and H (m) is the depth of the water column. We used measured time series of DO from 0.5 m above the sediment–water interface during the *first* hypoxic event at each site to compute the rate of DO consumption for the model calibration, that occurred between late April and mid-May 2019. We obtained values of −0.31% h^{-1}, −0.42% h^{-1}, and −0.54% h^{-1} in the Lower, Oaks, and Upper Arms, respectively (R^2 = [0.88–0.92]). We used the time series of DO next to the sediments after mid-May 2019 for model validation. We computed DO saturation using measured DO concentrations and lake water temperatures following Garcia and Gordon (1992). The coefficient of vertical eddy diffusivity K_z increased as L_N decreased. Depth average values of K_z were calculated from the 3-days filtered time series of lake temperature using the heat budget approach of Jassby and Powell (1975) to estimate the vertical turbulent transport only when the heat was mixed downwards. Values of K_z during upward transport were approximated using exponential regressions between K_z and buoyancy frequency, N (s^{-1}) (Text S2).

4.3. Buoyancy Frequency (N) Method

During the BIW method development, we observed an inverse relationship between DO saturation next to the sediments and the mean buoyancy frequency in the water column ($\bar{N}$) calculated as,

$$\bar{N}\left[s^{-1}\right] = \left(\sum_{z=1}^{z=z_{max}} \left(\sqrt{\frac{g}{\rho}\frac{\Delta\rho}{\Delta z}}\right)\right) \Big/ n_z \tag{8}$$

where ρ is the density in the water column at depth z, n_z is the number of depths in the water column where we measured temperature, z_{max} is the maximum depth, and $\Delta\rho/\Delta z$ is the vertical density gradient between two consecutive depths.

The *Buoyancy Frequency* method estimates DO saturation values at the sediment–water interface using $\bar{N}$ values. To minimize the number of input variables for this approach, we computed $\bar{N}'$ values, for which we only required surface and bottom lake temperatures, using Equation 8 and $z = 1$, $z = z_{max}$, $n_z = 2$. We estimated DO saturation values as,

$$\mathrm{DO}\left(\%\right) = \left[1 - \bar{N}'_{\mathrm{re\text{–}scaled}}\right] \times 100 \tag{9}$$

where $\bar{N}'_{\mathrm{re\text{–}scaled}}$ is the mean buoyancy frequency in the water column computed using only surface and bottom lake temperatures and re-scaled between 0 and 1. We found Equation 9 to be a good approximation since the coefficients of the linear regression $\mathrm{DO} = b + m\ \bar{N}'_{\mathrm{re\text{–}scaled}}$ were close to $b \sim 1$ and $m \sim -1$ ($b = 0.87 \pm 0.08$, $m = -0.96 \pm 0.05$, $R^2 = 0.43 \pm 0.09$) for the stratified periods or when $\bar{N}' > 0.015\ \mathrm{s}^{-1}$. This method would be considered as the 1-D method with "minimum requirements" or first-order approximation, albeit with some limitations, to estimate the length of the hypoxic events presented in this study. We found the results from this method acceptable for polymictic lakes because they captured the rapid changes in lake stratification as they modulate the DO availability.

5. Results

5.1. Lake Forcing

Meteorological forcing at Clear Lake led to noticeable patterns of daily heat fluxes over the year (Figure 3, S1, Text S3). SW_{net} and LE were the two dominant terms of the net surface heat flux, being source and sink terms, respectively. SE and LW_{net} fluxes were on average an order of magnitude lower. Daily heat fluxes changed seasonally and with the passage of cold/wet and warm/dry fronts. Daily SW_{net} was at a maximum in June ($2.5 \times 10^7\ \mathrm{J\ m^{-2}}$) and a minimum in December ($0.5 \times 10^7\ \mathrm{J\ m^{-2}}$). Cloudy periods lasted from 2-7 days with a mean reduction in SW_{net} of ~80% (Figure 3a). SE losses were negligible over the year except during extremely cold and windy episodes when SE ~ -5 x 10^6 J m^{-2}. Minor heat gains due to SE occurred under a thermally stable atmosphere (air temperature > lake surface temperature) and windy days. On average, daily LW_{net} was -7 x 10^6 J m^{-2} (Figure 3b). We did not observe large seasonal fluctuations for SE and LW_{net} because both heat fluxes were a function of the difference between the lake surface and air temperatures, which remained almost constant throughout the year (Figure S1). Mean LE values in winter and early spring were an order of magnitude lower than in summer and fall ($-1.5 \times 10^6\ \mathrm{J\ m^{-2}}$ and $-1.5 \times 10^7\ \mathrm{J\ m^{-2}}$, respectively). Large swings in LE occurred between consecutive days in the summer ($\sim \pm 3 \times 10^7\ \mathrm{J\ m^{-2}}$), mainly due to sustained high winds for 24 h, but also, as a result of low specific humidity (Figure 3c). Large differences in LE between basins are the result of the spatially very variable wind field across the lake (Figure S1).

As a result, the NSHF followed the combined trend of the SW_{net} and LE terms. NSHF values ranged between $-4 \times 10^7\ \mathrm{J\ m^{-2}}$ and 2 x 10^7 J m^{-2} (Figure 3d). On average, heat gain occurred between April and September, while heat losses dominated the heat budget from December to February. NSHF changed from being a source and a sink of heat almost daily during fall, spring, and winter months. The spatial variability across the lake of SW_{net}, SE, and LW_{net} was negligible, while more spatial variability occurred in the LE term, and thus, NSHF. Overall, LE losses were larger in the Oaks Arm than in the other two basins as a result of higher average wind speeds. The Upper Arm showed the largest annual NSHF of the three basins.

5.2. Lake Stratification and DO Dynamics

Lake surface temperatures in each basin varied seasonally (~28 °C in summer and ~8 °C in winter) and monthly during spring and summer as a result of multiple stratification and mixing events (Figures 4a, S2a, S3a). The water column was weakly stratified in winter (Dec-Feb) with a mean buoyancy frequency $\bar{N} < 0.005\ \mathrm{s}^{-1}$, while $\bar{N}$ values increased up to $0.015\ \mathrm{s}^{-1}$ during fall (Sep-Nov) and early spring (Mar-Apr). Late spring and summer stratification (May-Aug) was stronger, with $\bar{N}$ values above $0.02\ \mathrm{s}^{-1}$ for 2–3 weeks, followed by mixing events lasting 1–2 weeks. This periodicity in stratification and mixing is not as clear in the late fall and winter when the water column stratifies and mixes almost daily. Temperature

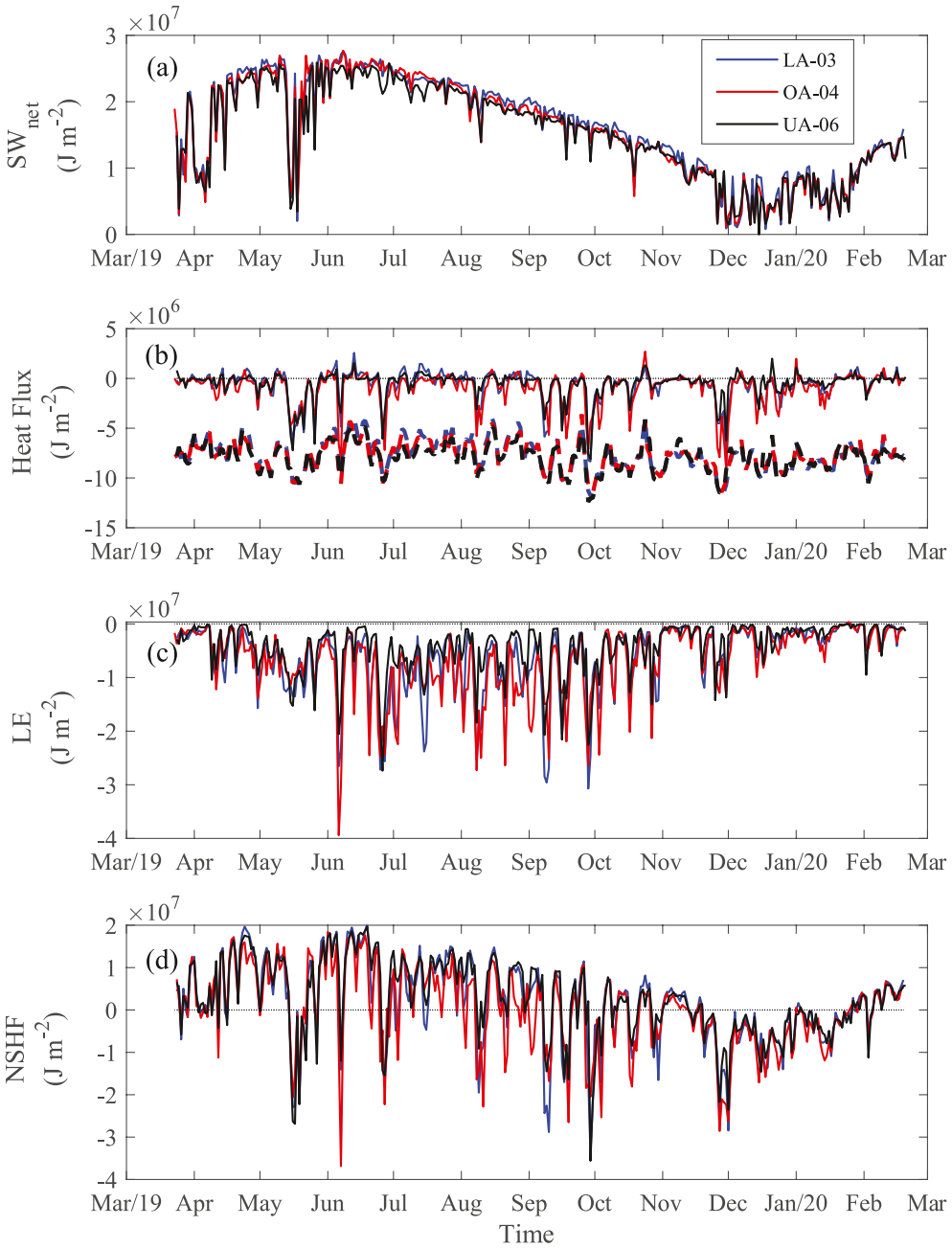

Figure 3. Daily surface heat fluxes for each basin: Lower Arm, LA-03 (blue), Oaks Arm, OA-04 (red), and Upper Arm, UA-06 (black): (a) Net shortwave radiation, (b) sensible heat flux (solid line), and net longwave radiation (dashed line), (c) latent heat flux, and (d) net surface heat flux.

gradients at depth tended to be stronger in the Upper Arm than in Oaks and Lower Arms during late summer and fall, most likely due to spatially variable NSHF as a result of the wind field across the lake.

The strength of the stratification was inversely related to DO concentrations near the sediments (Figures 4b, S2b, S3b). During spring and summer, near-bottom DO concentrations were progressively depleted for 10–15 days after the onset of stratification or $\bar{N} > 0.015\ s^{-1}$. If the near-sediment water column remained isolated for more than 2 weeks, fully anoxic conditions (0 mg L^{-1}) developed next to the sediment–water interface. We observed three pronounced hypoxic events in the Lower and Oaks Arm basins, and four events in the Upper Arm. The water column fully re-oxygenated in less than 24-h as a result of full mix-

Table 4
Length of the Hypoxic Periods in Days for the Different Hypoxic Events Occurring in the Three Basins Using Four Different Dissolved Oxygen Concentration Thresholds (1, 2, 3, and 4 mg L^{-1}) and Four Methods: Direct Observation of Dissolved Oxygen Concentrations Next to the Sediments (DO), the Birge-Winkler (BIW) Method, the Lake Number (L_N) Method, and the Buoyancy Frequency (N) Method

		Lower Arm				Oaks Arm				Upper Arm			
DO threshold	Hypoxic Event #	DO	BIW	L_N	N	DO	BIW	L_N	N	DO	BIW	L_N	N
1 mg L^{-1}	1	5	8	3		2	6	1		10	12	10	
	2	10	10	9		7	6	8		9	10	9	
	3	3	5	2		4	6	3		16	20	16	
	4									4	7	5	
2 mg L^{-1}	1	9	13	7		9	12	8		12	15	12	
	2	11	11	11	4	9	8	9	5	10	11	10	
	3	8	12	4		6	9	5		18	22	17	
	4									13	10	6	
3 mg L^{-1}	1	11	15	10	8	12	17	11	5	15	16	15	5
	2	14	13	12	8	14	10	13	12	11	12	11	8
	3	8	11	9		7	10	10		18	17	18	
	4									14	13	14	
4 mg L^{-1}	1	13	16	14	20	13	18	13	19	16	16	16	21
	2	15	13	15	16	14	14	14	14	13	12	13	15
	3	11	15	10	5	11	5	11	7	20	17	20	
	4									16	14	17	

Grayed sections due to the inaccuracy of the *N* method and the number of hypoxic events in the smaller arms.
RMSE for BIW, L_N, and *N* methods are [2.9, 1.4, 5.24] days, respectively.
NSE for BIW, L_N, and *N* methods are [0.40 (good), 0.65 (very good), 0.21 (good)], respectively.
Note. The difference in the length of the hypoxic periods between DO measurements and other methods is shown in Table S2.

ing and lasted for about a week if mixing conditions persisted (i.e., low NSHF). The onset of hypoxia and re-oxygenation in spring and summer varied between 1 to 10 days between basins, with longer and more frequent hypoxic events in the Upper Arm, while events were fairly synchronized in the Lower and Oaks Arm (Table 4, DO column). During fall, DO values ranged between 3 and 7 mg L^{-1} due to a sequence of short and weak stratification and mixing events. Brief hypoxic events occurred in the Upper Arm during fall as a result of the stronger stratification in this basin. DO concentrations continuously increased in winter reaching values ~10 mg L^{-1} due to a combination of colder water temperatures and more gas exchange with the atmosphere.

5.3. Birge-Winkler Method and Hypoxia

The *Birge-Winkler* method was used to estimate the onset and duration of the hypoxic events in the three basins (Figures 4c, 4d, S2c-d, S3c-d). The trend of the BIW energy term and its value at the onset of the hypoxia (BIW_{c1}) provided a proxy of the DO trend next to the sediments. The trend of the BIW energy term presented similar patterns in spring and summer in the Oaks and Lower Arm and in each basin predicted 3 hypoxic events lasting 2–3 weeks. Oaks Arm basin gained significantly less heat during fall and winter. Heat losses in the Upper Arm were minimal in the summer compared to the other two basins which yielded one additional hypoxic event (total of four) compared to the other two basins. The cut-off energy term or BIW_{c1} changed ~20% between basins and up to 4% depending on the DO threshold we used to define the beginning of the hypoxic period, ranging between 1 and 4 mg L^{-1} (Table 3). Once that BIW_{c1} was defined, the *Birge-Winkler* method predicted the onset of the hypoxic events with an averaged error of ±3 days when compared with direct measurements of DO next to the sediments (Table 4 – DO and BIW columns, and Table S2), and a Nash-Sutcliffe model efficiency coefficient reflecting good fit (NSE = 0.4).

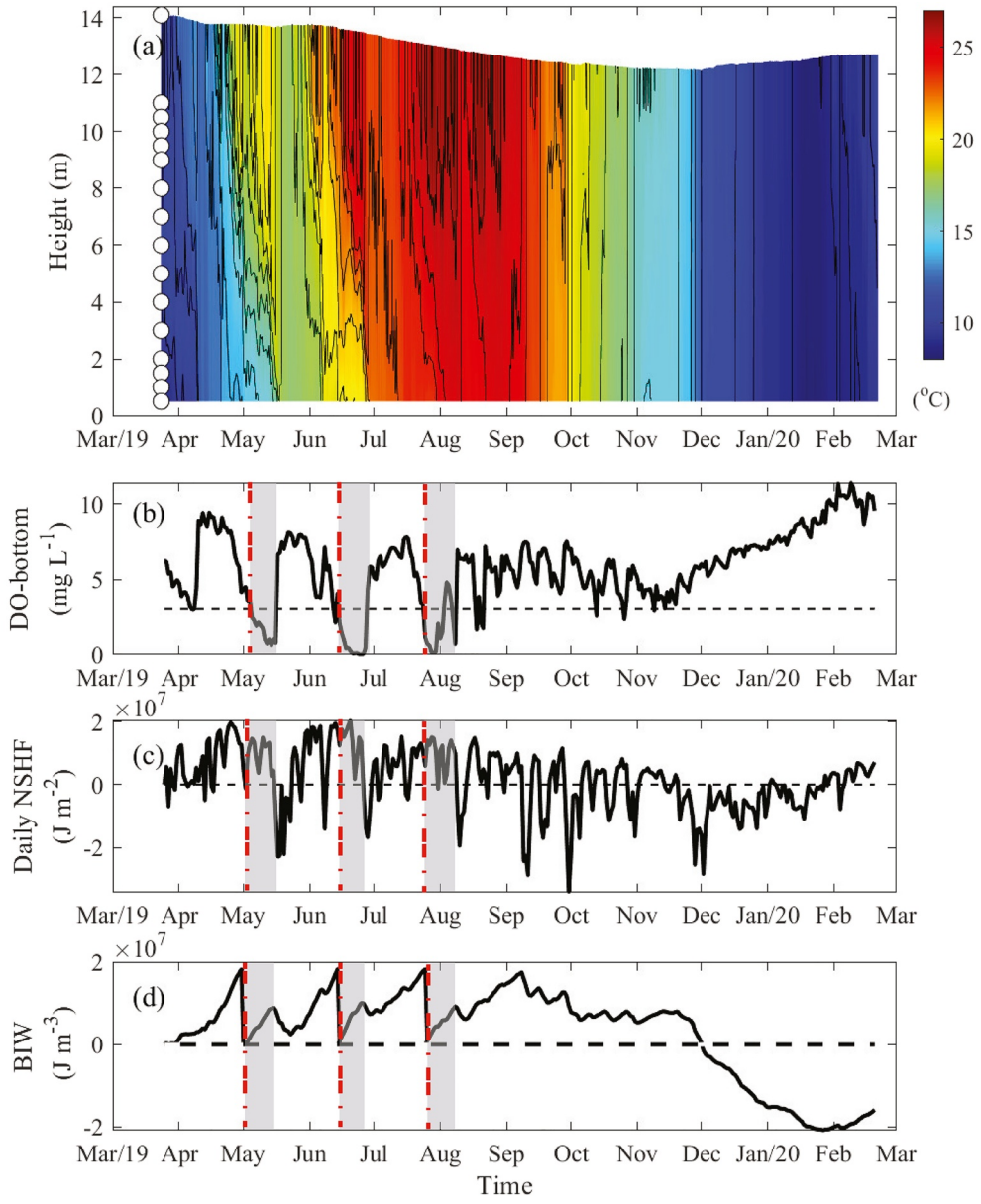

Figure 4. Lower Arm, LA-03. (a) Four-hour average lake temperature presented as height off the bottom, with isotherms every 1 °C. White dots mark the depths of the instruments. (b) Daily filtered dissolved oxygen concentrations at 0.5 m above the bottom. Dashed line at 3 mg L^{-1}. Red dotted-dashed lines mark the onset of hypoxic events (DO < 3 mg L^{-1}). Gray squares indicate the duration of hypoxia. (c) NSHF. (d) BIW energy term with BIW_{c1} of 1.8×10^7 J m^{-3} and a DO_{thr} of 3 mg L^{-1}.

5.4. Lake Number Method and Hypoxia

With the inverse relationship between DO and L_N values, we were able to use L_N to quantify the extent of mixing and stratification in the three basins and also predict the changes of DO next to the sediments (Figure 5, S4, S5). We computed the length of the hypoxic events and compared them with the measured DO values and the BIW method results (Table 4). Decreasing DO was strongly linked to high L_N values due to reduced mixing and bottom isolation. DO was gradually depleted over ~2 weeks after the onset of stratification. Provided L_N remained high, DO saturation remained near zero. Conversely, high values of vertical eddy diffusivity K_z were associated with high DO saturation values as a result of wind-driven mixing.

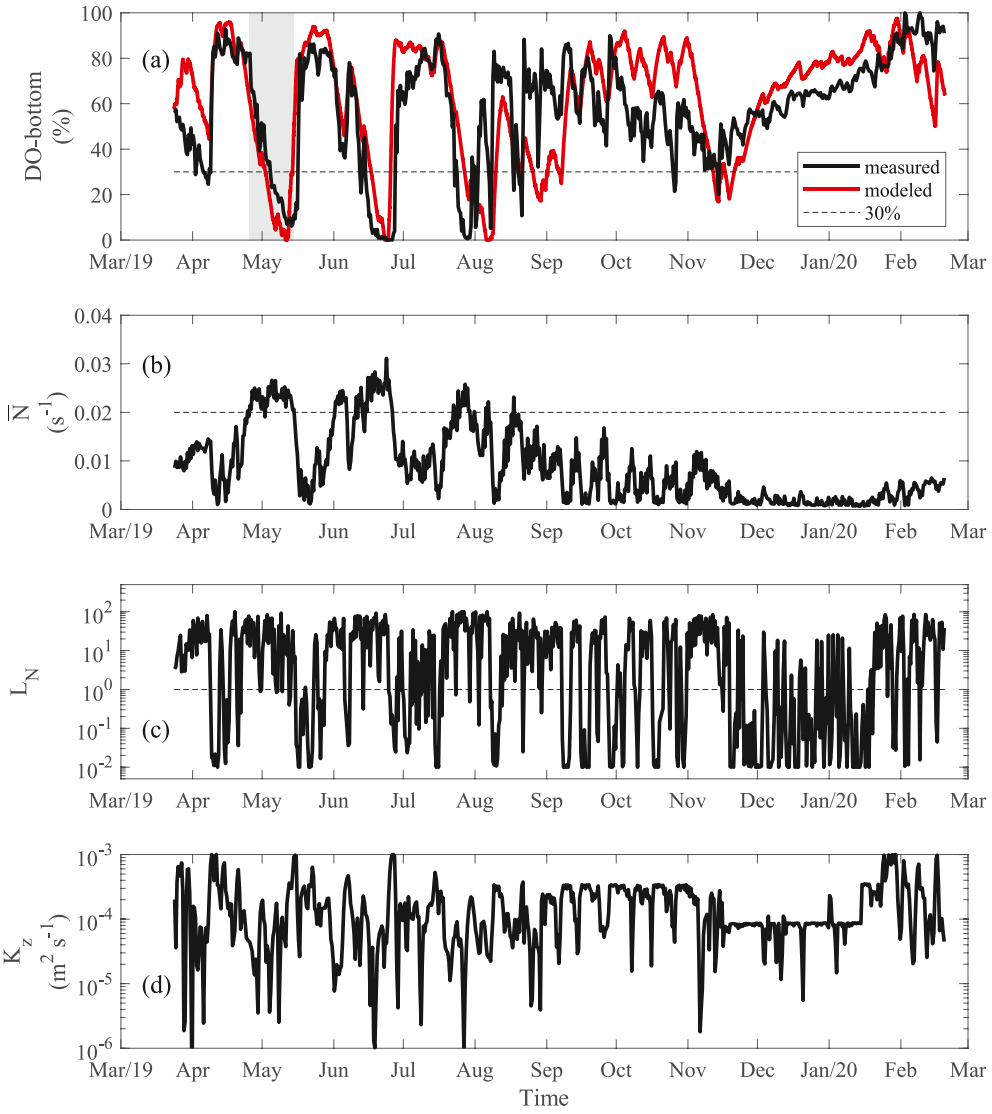

Figure 5. Lower Arm, LA-03. Twelve-hour average time series of (a) measured DO (%) at 0.5 m above the bottom in black, and modeled values in red using the *Lake Number* method. Dashed line marks 30% saturation. The gray area marks the calibration period (b) Mean buoyancy frequency ($\overline{N}$) in the water column. Dashed line marks 0.02 s^{-1}. (c) Lake Number (L_N) values. Dashed line marks $L_N = 1$. (d) Depth-average vertical eddy diffusivity (K_z).

Calculated values of DO saturation using the L_N method show good agreement with the measured values, particularly during spring and summer (Apr-Aug) when $\overline{N} > 0.015$ s^{-1} (R^2 = [0.45–0.66]). The L_N approach tended to overestimate DO values in fall and winter (Sep-Feb). However, this approach predicted the onset of the hypoxic events with an error of ±1 day when compared with direct measurements of DO next to the sediments and a Nash-Sutcliffe model efficiency coefficient indicative of a very good fit (NSE = 0.65) (Tables 4 and S2). Thus, the L_N approach provides a more accurate estimate of the extent of hypoxic events than the BIW method. Nevertheless, computing L_N values requires a substantially larger number of measured input variables, both in-lake, and meteorological data.

5.5. Buoyancy Frequency Method and Hypoxia

We used the inverse relationship between the mean buoyancy frequency in the water column ($\overline{N}'$) and the DO concentration next to the sediments to predict hypoxia (Figure 6). This method requires the minimum input data of the three methods: lake surface and bottom temperatures to compute $\overline{N}'$. Results showed a

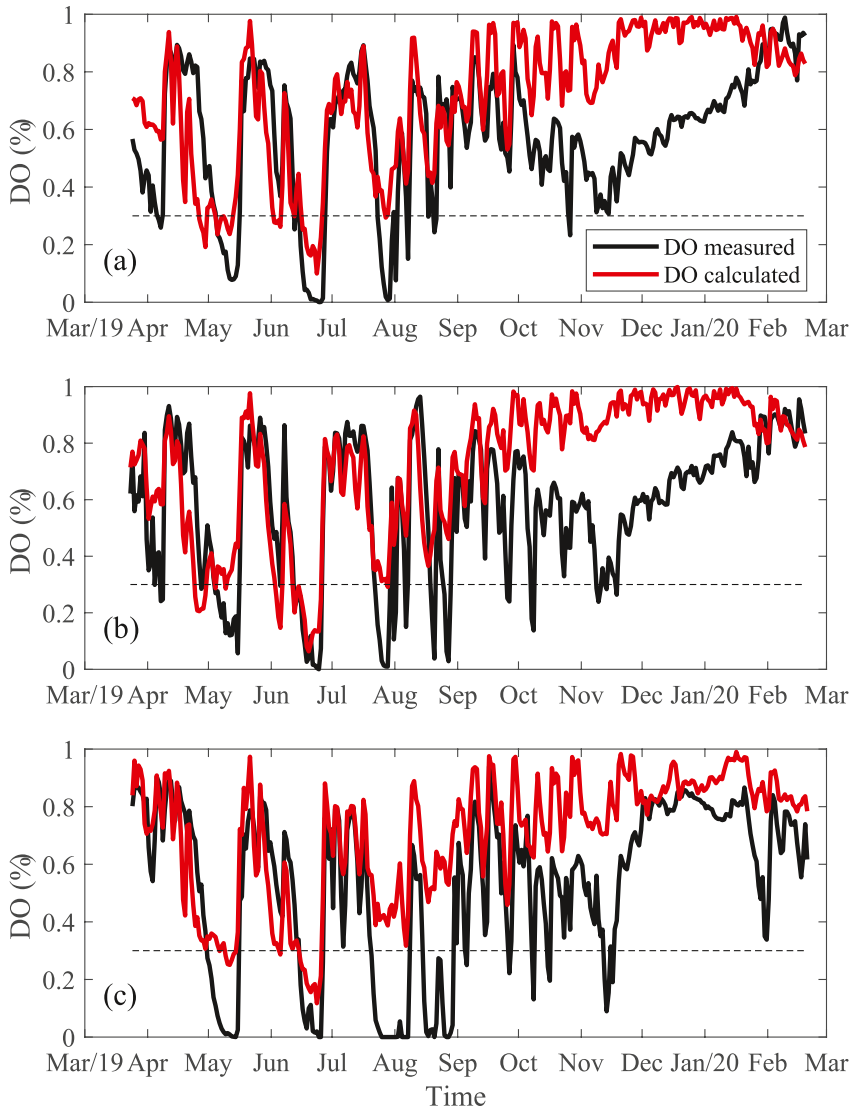

Figure 6. Time series of dissolved oxygen saturation measured (black) and calculated (red) using the *Buoyancy Frequency* (N) method for (a) Lower Arm, LA-03, (b) Oaks Arm, OA-04, and (c) Upper Arm, UA-06.

reasonable agreement between measured and calculated DO saturation values next to the sediments during spring and summer ($R^2 = 0.43 \pm 0.09$ in the 3 basins), but not in fall and winter ($R^2 = 0.18 \pm 0.11$ in the 3 basins). The correlation between measured and computed DO values improved very little when $\bar{N}$ values were more precisely calculated using multiple lake temperature measurements throughout the water column as in Equation 8 (e.g., $R^2 = 0.46 \pm 0.08$ in the 3 basins). This method predicted the onset and length of the hypoxic events with an error of ±5 days when compared with direct measurements of DO, but only for DO thresholds of 3 and 4 mg L^{-1} (Tables 4 and S2, NSE = 0.21). We were unable to reproduce low levels of DO using the buoyancy frequency method, hence, we were not capable of predicting hypoxic events of DO ≤ 2 mg L^{-1}.

Table 5
Summary of the Input Data, Advantages, and Disadvantages of the Three Methods to Predict the Duration of Hypoxic Events.

Method	Input data	Advantages	Disadvantages
Birge-Winkler (BIW) Method	*Parameters* - Lake latitude - Lake elevation or atmospheric pressure - Wind sensor height - Maximum lake depth - Threshold of accumulated BIW energy term at the onset of the hypoxic event, BIW_{c1} *Hourly time series* - Lake surface temperature - Air temperature - Relative humidity - Incoming shortwave radiation - Wind speed	- *Input data* parameters and time series are generally *available* for most study sites - *Estimates* of the *length of the hypoxic events are* on par *with* those from direct DO measurements at the sediment–water interface	- Values of DO next to the sediments are not directly computed - The calibration parameter (BIW_{c1}) requires *time series of DO.* This parameter will change depending on the selected DO threshold
Lake Number (L_N) Method	*Parameters* - Lake latitude - Lake elevation or atmospheric pressure - Wind sensor height - Maximum lake depth - Lake hypsography - Depletion rate of DO next to the sediments *Hourly time series* - Lake temperature at multiple depths - Air temperature - Relative humidity - Incoming shortwave radiation - Wind speed - Depth average eddy diffusivity, K_z - Surface DO	- Calculation of *actual DO* values next to the sediments (%) - *Most accurate estimates* of the length of hypoxic events	- *The largest amount of input data* (both parameters and time series) - *Careful calibration* against DO measurements to obtain meaningful results
Buoyancy Frequency (N) Method	*Hourly time series* - Lake surface and bottom temperature	- *Minimum amount of input data* - Calculation of *actual DO* values next to the sediments (%)	- Reliable results only when $N > 0.015$ s^{-1} - Reliable results only for *high thresholds of DO* to define hypoxia (>2 mg L^{-1})

Note. Model calibration requires time series of dissolved oxygen at the sediment–water interface.

6. Discussion

We predicted the onset and duration of hypoxic events for a full stratified season in the three basins of Clear Lake using the *Lake Number* method, and two original approaches, the *Birge-Winkler* and the *Buoyancy Frequency* methods. The required input data, advantages, and disadvantages of each method are summarized in Table 5.

The new BIW method uses daily net surface heat fluxes to estimate the onset and duration of hypoxic events in polymictic lakes, and requires minimal input data, calibration, and validation. The calibration of the BIW method needs DO data next to the sediments, and the cut-off parameter BIW_{c1} defining the beginning of the hypoxic period which changes depending on the DO thresholds used to define hypoxia (Table 3). This method was shown to be a simple and effective tool to determine when and for how long hypoxic events occur in polymictic lakes where meteorology is the main driver of the extent of these events, with ±3 days of uncertainty (Tables 4 and S2). On average, this uncertainty represents between 10% and 15% error of the observed hypoxic periods (2–3 weeks). An advantage of the BIW method is that, unlike the L_N method, it does not require hypsographic data. The accuracy in the prediction of the length of hypoxia only improved by two days when using the L_N method which considers both stratification and meteorological forcing, being the Nash-Sutcliffe model efficiency coefficient or NSE = 0.4 (good) for BIW method and NSE = 0.65 (very good) for L_N method. Although the L_N method requires a substantial amount of input data and calibration parameters, it yields explicit estimates of lake DO values near the sediment–water interface. In contrast, the *N* method is a simplified version of the BIW which considers only lake stratification and predicts DO saturation values at the sediment–water interface. However, predictions of the length of the hypoxic events using the *N* method had the largest error (±5 days, NSE = 0.21), only worked when the stratification was significant ($\overline{N} > 0.015\ s^{-1}$) and the DO threshold of hypoxia had to be above 2 mg L^{-1}.

The BIW method balances the logistical demand for acquiring data with the reliability of the results, making it a powerful and comparatively easy tool. It was developed using data from the three individual basins of Clear Lake for calibration and validation, it can be readily generalizable to other polymictic water bodies.

6.1. Generalized Birge-Winkler (BIW) Method

The broad application of the BIW method across a variety of lakes requires the characterization of a variety of fundamental lake processes in addition to meteorological forcing. For example, shallow polymictic lakes can mix to the bottom frequently whereas deep dimictic lakes will undergo seasonal stratification and overturn (Kirillin & Shatwell, 2016). Lake stratification is strongly dependent on air temperature, wind speed, and basin morphometric characteristics, such as maximum depth and surface area (Adrian et al., 2009; Kraemer et al., 2015). Mictic state and stratification dynamics will directly impact seasonal rates of DO consumption, and, in turn, will drive the availability of nutrients at the sediment–water interface (Nürnberg, 2002). The rate of DO consumption affects the calibration of the BIW method, which can be directly measured or estimated as a function of factors such as lake trophic state or organic matter loads from the watershed (Del Giorgio & Williams, 2005).

The generalization of the BIW method requires calibration of the BIW_{c1} value at the onset of the hypoxic period. The BIW energy term has already been normalized by the maximum depth of the basin. We developed a linear regression between BIW_{c1} values and the ratio between the surface area (A_0) and the daily rate of DO consumption at the sediment-water interface (a = [7.4–13] % d^{-1}), which yielded the following relationship:

$$BIW_{c1}\left[\mathrm{J\ m^{-3}}\right] = b + m\left(\frac{A_0\left[\mathrm{m^2}\right]}{a\left[\%\ \mathrm{d^{-1}}\right]}\right) \tag{10}$$

where $b = 1.42 \times 10^7$ J m^{-3} and $m = 1.20$ J m^{-5} d^{-1} ($R^2 = 0.95$, $p < 0.01$, statistically significant, 12 data points) when the DO threshold varied between 1 and 4 mg L^{-1}. The use of Equation 10 to estimate BIW_{c1} yielded errors of less than 1 day when predicting the onset and length of hypoxia in our study sites. This is a first-order approximation of this model that would be further refined with the inclusion of secondary

variables in the regression. For example, DO consumption in monomictic or dimictic lakes may change over time due to limited overturn periods. DO consumption will also change depending on the trophic state of the lake and the validity of this method should be tested in mesotrophic systems. Inflows may add or remove energy as heat to the system and impact the lake stratification, and thus, values of the calibration parameter BIW_{c1}. Another energy source that may modify BIW_{c1} is the artificial aeration. Energy may be also redistributing in the system due to internal waves. As a result, the inclusion of secondary variables in Equation 10 will depend on the dominance of the process they represent.

6.2. Uses of the BIW Method

Lake stratification and oxygen are key for ecological processes and water quality in lakes. Strong lake stratification intensifies oxygen depletion which reduces fish habitat, promotes nuisance HABs, and favors internal nutrient loading (Diaz & Rosenberg, 2008; Orihel et al., 2017; Paerl & Paul, 2012). Simple methods to predict hypoxia, such as the BIW or *N* methods, can be extremely powerful at relatively low cost to address these aquatic ecological challenges.

The reduction of fish habitat due to hypoxia/anoxia is a growing concern (Feyrer et al., 2020; Goldman & Wetzel, 1963). We suggest that the BIW method can be modified to function as an indicator of fish stress resulting from hypoxia. For example, the ratio between the heat content per unit volume in the lake (the BIW energy term) and the shear energy in the water per unit volume (product between lake density ρ and the square of the shear velocity on the lake surface u_*) represents a balance between stabilizing and destabilizing forces, which together control rates of DO depletion and replenishment within the water column, and thus can be calibrated to reflect stress or potential mortality of different fishes.

Hypoxia also favors internal nutrient loading from the sediments (Welch & Cooke, 1995). Sediment nutrient release is directly related to the length of the DO depleted period and the sediment area exposed to low DO concentrations (Orihel et al., 2017). When properly calibrated, the BIW method estimates the length of the hypoxic period without requiring *in situ* measurement of DO, which will inform internal nutrient loading calculations. For Clear Lake, this model proves predictions of the extent of hypoxia with an uncertainty of ~15%, which translates into a similar error for the internal loading estimates.

Finally, the direct effects of climate change on lake stratification have been broadly recognized (Toffolon et al., 2020; Woolway & Merchant, 2019). Changes over time in air temperature, wind speeds, and relative humidity will alter surface temperatures in lakes and thermal stratification dynamics (Adrian et al., 2009), while lake morphometry influences the response of lake stratification to changing air temperatures and wind speeds (Kraemer et al., 2015). Wind magnitude directly affects the NSHF, and thus, the BIW energy term, but wind also affects mixing as expressed by the Lake Number. Since the BIW method takes into account the effects of changing air temperature, wind, and lake morphometry (depth and area), we believe it will provide critical information to guide management and restoration measurements in Clear Lake and other lakes with similar ecological challenges due to hypoxia.

6.3. Uncertainties and Future Lines of Research

This work has explored and discussed simple one-dimensional (1-D) methods to predict hypoxia in shallow lakes. We have proved these methods can provide a reasonable first-order approximation of the onset of hypoxic events in water bodies where only vertical changes are of interest. However, a two-dimensional (2-D) approach may be required if the system exhibits both longitudinal and vertical hydrodynamic and water quality gradients, such as CE-QUAL model (Cole & Wells, 1995). These tools can be particularly effective in elongated deep systems where lateral gradients are not appreciable. Nevertheless, this assumption may not be sufficient to reproduce three-dimensional (3-D) transport processes in large systems with complex bathymetry, where lateral changes can be significant. Different transport processes have been studied in multibasin lakes, such as internal waves, advection, or rotational transport (Flood et al., 2020; Imam et al., 2019). Results are generally very specific for each site study where a 3-D model has been utilized to depict the distribution of particles and solutes in the water body (Valipour et al., 2019). The outputs of more complex 3-D models could inform potential changes in lake DO concentrations at different temporal and spatial scales

than those given by methods detailed in this work but come at the cost of significant processing overhead. Given growing concerns of DO depletion in the water column as a result of the system eutrophication and warming climate (Schindler et al., 2016), it is important to have potential tools, from 1-D to 3-D, to study each of these problems even if the performance of these tools is still an active area of research (Toffolon & Serafini, 2013).

7. Conclusions

Predicting the DO drawdown in lakes normally requires intensive data and complex models, which are often not available or affordable for many lakes. To overcome this challenge, we developed and tested the *Birge-Winkler* (BIW) method to forecast the onset and duration of hypoxic events in polymictic lakes. The calibration of this method required lake DO time series adjacent to the sediments, but its validation proved the method to be accurate for predicting the onset of hypoxia without computing or measuring actual lake DO values. The good performance of the BIW method indicates that meteorological forcing is the main driver of hypoxia in polymictic lakes. We suggest this method can be calibrated for use in other shallow lakes, providing a useful and cost-effective decision-making tool.

Data Availability Statement

Datasets for this research are available in this data citation reference: Cortés, A. & Schladow, S. G. (2020). Lake temperature, dissolved oxygen and meteorological data in Clear, CA, USA (2019–2020). Knowledge Network for Biocomplexity. doi: https://doi.org/10.5063/F1C827P7.

Acknowledgments
The authors appreciate the support of the UC Davis TERC field team Brant Allen, Brandon Berry, Katie Senft, and Raph Townsend and James Fitzgerald from the Bodega Marine Laboratory. The authors thank Angela DePalma-Dow from Lake County Department of Water Resources for her advice and support in the field. The authors acknowledge the efforts of Shohei Watanabe and Dean Bunn in archiving real-time data, and our UC Davis TERC laboratory team of Anne Liston, Steven Sesma, Tina Hammell, Lindsay Vaughan, and Lidia Tanaka. Carmen Bedke was the project administrator. The authors are thankful for the net surface heat flux code developed in MacIntyre Lab. This study was funded by the California Department of Fish and Wildlife. The work was conducted on behalf of the Blue Ribbon Committee for the Rehabilitation of Clear Lake (https://resources.ca.gov/Initiatives/Blue-Ribbon-Committee-for-the-Rehabilitation-of-Clear-Lake).

References

Adrian, R., O'Reilly, C. M., Zagarese, H., Baines, S. B., Hessen, D. O., Keller, W., et al. (2009). Lakes as sentinels of climate change. *Limnology & Oceanography*, *54*(6), 2283–2297. https://doi.org/10.4319/lo.2009.54.6_part_2.2283

Allen, J. I., Holt, J. T., Blackford, J., & Proctor, R. (2007). Error quantification of a high-resolution coupled hydrodynamic-ecosystem coastal-ocean model: Part 2. Chlorophyll-a, nutrients and SPM. *Journal of Marine Systems*, *68*(3–4), 381–404. https://doi.org/10.1016/j.jmarsys.2007.01.005

Biddanda, B. A., Weinke, A. D., Kendall, S. T., Gereaux, L. C., Holcomb, T. M., Snider, M. J., et al. (2018). Chronicles of hypoxia: Time-series buoy observations reveal annually recurring seasonal basin-wide hypoxia in Muskegon Lake - A Great Lakes estuary. *Journal of Great Lakes Research*, *44*(2), 219–229. https://doi.org/10.1016/j.jglr.2017.12.008

Bouffard, D., Ackerman, J. D., & Boegman, L. (2013). Factors affecting the development and dynamics of hypoxia in a large shallow stratified lake: Hourly to seasonal patterns. *Journal of Geophysical Research: Water Resources Research*, *49*(5), 2380–2394. https://doi.org/10.1002/wrcr.20241

Chen, C.-T. A., & Millero, F. J. (1986). Thermodynamic properties for natural waters covering only the limnological range1. *Limnology & Oceanography*, *31*(3), 657–662. https://doi.org/10.4319/lo.1986.31.3.0657

Cole, T. M., & Wells, S. A. (1995). CE-QUAL-W2: A Two-dimensional, laterally averaged, hydrodynamic and water quality model. *Vicksburg*.

Del Giorgio, P., & Williams, P. (2005). Respiration in aquatic ecosystems. Respiration in aquatic ecosystems. Oxford University Press. https://doi.org/10.1093/acprof:oso/9780198527084.001.0001

Diaz, R. J., & Rosenberg, R. (2008). Spreading dead zones and consequences for marine ecosystems. *Science*, *321*(5891), 926–929. https://doi.org/10.1126/science.1156401

Feyrer, F., Young, M., Patton, O., & Ayers, D. (2020). Dissolved oxygen controls summer habitat of Clear Lake Hitch (Lavinia exilicauda chi), an imperiled potamodromous cyprinid. *Ecology of Freshwater Fish*, *29*(2), 188–196. https://doi.org/10.1111/eff.12505

Flood, B., Wells, M., Dunlop, E., & Young, J. (2020). Internal waves pump waters in and out of a deep coastal embayment of a large lake. *Limnology & Oceanography*, *65*(2), 205–223. https://doi.org/10.1002/lno.11292

Garcia, H. E., & Gordon, L. I. (1992). Oxygen solubility in seawater: Better fitting equations. *Limnology & Oceanography*, *37*(6), 1307–1312. https://doi.org/10.4319/lo.1992.37.6.1307

Goldman, C. R., & Wetzel, R. G. (1963). A study of the primary productivity of Clear Lake, Lake County California. *Ecology*, *44*, 283–294. https://doi.org/10.2307/1932175

Hicks, B. B. (1975). A procedure for the formulation of bulk transfer coefficients over water. *Boundary-Layer Meteorology*, *8*, 515–524. https://doi.org/10.1007/bf02153568

Imam, Y. E., Laval, B., Pieters, R., & Lawrence, G. (2019). The baroclinic response to wind in a multiarm multibasin reservoir. *Limnology & Oceanography*, *65*, 582–600. https://doi.org/10.1002/lno.11328

Imberger, J. (1985). The diurnal mixed layer1. *Limnology & Oceanography*, *30*(4), 737–770. https://doi.org/10.4319/lo.1985.30.4.0737

Jassby, A., & Powell, T. (1975). Vertical patterns of eddy diffusion during stratification in Castle Lake, California1. *Limnology & Oceanography*, *20*(July), 530–543. https://doi.org/10.4319/lo.1975.20.4.0530

Kalff, J. (2002). *Limnology. Inland water ecosystems*. Prentice Hall. https://doi.org/10.2118/74039-ms

Kirillin, G., & Shatwell, T. (2016). Generalized scaling of seasonal thermal stratification in lakes. *Earth-Science Reviews*, *161*, 179–190. https://doi.org/10.1016/j.earscirev.2016.08.008

Kraemer, B. M., Anneville, O., Chandra, S., Dix, M., Kuusisto, E., Livingstone, D. M., et al. (2015). Morphometry and average temperature affect lake stratification responses to climate change. *Geophysical Research Letters*, *42*, 4981–4988. https://doi.org/10.1002/2015GL064097

Leon, L. F., Smith, R. E. H., Hipsey, M. R., Bocaniov, S. A., Higgins, S. N., Hecky, R. E., et al. (2011). Application of a 3D hydrodynamic-biological model for seasonal and spatial dynamics of water quality and phytoplankton in Lake Erie. *Journal of Great Lakes Research*, *37*(1), 41–53. https://doi.org/10.1016/j.jglr.2010.12.007

MacIntyre, S., Romero, J. R., & Kling, G. W. (2002). Spatial-temporal variability in surface layer deepening and lateral advection in an embayment of Lake Victoria, East Africa. *Limnology & Oceanography*, *47*(3), 656–671. https://doi.org/10.4319/lo.2002.47.3.0656

Magee, M. R., & Wu, C. H. (2017). Response of water temperatures and stratification to changing climate in three lakes with different morphometry. *Hydrology and Earth System Sciences*, *21*(12), 6253–6274. https://doi.org/10.5194/hess-21-6253-2017

Martinez, D., & Anderson, M. A. (2013). Methane production and ebullition in a shallow, artificially aerated, eutrophic temperate lake (Lake Elsinore, CA). The *Science of the Total Environment*, *454–455*, 457–465. https://doi.org/10.1016/j.scitotenv.2013.03.040

Martin, J. L., & McCutcheon, S. C. (1999). *Hydrodynamics and transport for water quality modeling*. CRC Press.

Matzinger, A., Müller, B., Niederhauser, P., Schmid, M., & Wüest, A. (2010). Hypolimnetic oxygen consumption by sediment-based reduced substances in former eutrophic lakes. *Limnology & Oceanography*, *55*(5), 2073–2084. https://doi.org/10.4319/lo.2010.55.5.2073

Müller, B., Bryant, L. D., Matzinger, A., & Wüest, A. (2012). Hypolimnetic oxygen depletion in eutrophic lakes. *Environmental Science & Technology*, *46*(18), 9964–9971. https://doi.org/10.1021/es301422r

Müller, B., Steinsberger, T., Schwefel, R., Gächter, R., Sturm, M., & Wüest, A. (2019). Oxygen consumption in seasonally stratified lakes decreases only below a marginal phosphorus threshold. *Scientific Reports*, *9*(1), 1–7. https://doi.org/10.1038/s41598-019-54486-3

Neumann, G., & Pierson, W. J. (1966). *Principles of physical oceanography*. Prentice-Hall.

Nürnberg, G. K. (2002). Quantification of oxygen depletion in lakes and reservoirs with the hypoxic factor. *Lake and Reservoir Management*, *18*(4), 299–306. https://doi.org/10.1080/07438140209353936

Nürnberg, G. K., LaZerte, B. D., Loh, P. S., & Molot, L. A. (2013). Quantification of internal phosphorus load in large, partially polymictic and mesotrophic Lake Simcoe, Ontario. *Journal of Great Lakes Research*, *39*(2), 271–279. https://doi.org/10.1016/j.jglr.2013.03.017

Orihel, D. M., Baulch, H. M., Casson, N. J., North, R. L., Parsons, C. T., Seckar, D. C. M., & Venkiteswaran, J. J. (2017). Internal phosphorus loading in canadian fresh waters: A critical review and data analysis. *Canadian Journal of Fisheries and Aquatic Sciences*, *74*(12), 2005–2029. https://doi.org/10.1139/cjfas-2016-0500

Paerl, H. W., & Paul, V. J. (2012). Climate change: Links to global expansion of harmful cyanobacteria. *Water Research*, *46*(5), 1349–1363. https://doi.org/10.1016/j.watres.2011.08.002

Peña, M. A., Katsev, S., Oguz, T., & Gilbert, D. (2010). Modeling dissolved oxygen dynamics and hypoxia. *Biogeosciences*, *7*(3), 933–957. https://doi.org/10.5194/bg-7-933-2010

Qin, B., Zhu, G., Gao, G., Zhang, Y., Li, W., Paerl, H. W., & Carmichael, W. W. (2010). A drinking water crisis in Lake Taihu, China: Linkage to climatic variability and lake management. *Environmental Management*, *45*(1), 105–112. https://doi.org/10.1007/s00267-009-9393-6

Richerson, P. J., Suchanek, T. H., Zierenberg, R. A., Osleger, D. A., Heyvaert, A. C., Slotton, D. G., et al. (2008). Anthropogenic stressors and changes in the Clear Lake ecosystem as recorded in sediment cores. *Ecological Applications*, *18*(8), A257–A283. https://doi.org/10.1890/06-1458.1

Richerson, P., Suchanek, T. H., & Why, S. (1994). The causes and control of algal blooms in Clear Lake. Retrieved from https://www.researchgate.net/publication/242643163_THE_CAUSES_AND_CONTROL_OF_ALGAL_BLOOMS_IN_CLEAR_LAKE_Clean_Lakes_DiagnosticFeasibility_Study_For_Clear_Lake_California

Robertson, D. M., & Imberger, J. (1994). Lake number, a quantitative indicator of mixing used to estimate changes in dissolved oxygen. *Internationale Revue der gesamten Hydrobiologie und Hydrographie*, *79*(2), 159–176. https://doi.org/10.1002/iroh.19940790202

Rucinski, D. K., Beletsky, D., DePinto, J. V., Schwab, D. J., & Scavia, D. (2010). A simple 1-dimensional, climate based dissolved oxygen model for the central basin of Lake Erie. *Journal of Great Lakes Research*, *36*(3), 465–476. https://doi.org/10.1016/j.jglr.2010.06.002

Rueda, F. J., Geoffrey, S. G., & Clark, J. F. (2008). Mechanisms of contaminant transport in a multi-basin lake. *Ecological Applications*, *18*(8), A72–A87. https://doi.org/10.1890/06-1617.1

Rueda, F. J., Schladow, S. G., Monismith, S. G., & Stacey, M. T. (2003). Dynamics of Large Polymictic Lake. I: Field Observations. *Journal of Hydraulic Engineering*, *129*(2), 82–91. https://doi.org/10.1061/(ASCE)0733-9429

Schindler, D. W., Carpenter, S. R., Chapra, S. C., Hecky, R. E., & Orihel, D. M. (2016). Reducing phosphorus to curb lake eutrophication is a success. *Environmental Science & Technology*, *50*(17), 8923–8929. https://doi.org/10.1021/acs.est.6b02204

Schladow, S. G., & Hamilton, D. P. (1997). Prediction of water quality in lakes and reservoirs: Part II - Model calibration, sensitivity analysis and application. *Ecological Modelling*, *96*(1–3), 111–123. https://doi.org/10.1016/S0304-3800(96)00063-4

Suchanek, T. H., Eagles-Smith, C. A., Slotton, D. G., Harner, E. J., Colwell, A. E., Anderson, N. L., et al. (2008). Spatiotemporal trends in fish mercury from a mine-dominated ecosystem: Clear Lake, California. *Ecological Applications*, *18*, A177–A195. https://doi.org/10.1890/06-1900.1

Taranu, Z. E., Köster, D., Hall, R. I., Charette, T., Forrest, F., Cwynar, L. C., & Gregory-Eaves, I. (2010). Contrasting responses of dimictic and polymictic lakes to environmental change: A spatial and temporal study. *Aquatic Sciences*, *72*(1), 97–115. https://doi.org/10.1007/s00027-009-0120-4

Thompson, L. C., Giusti, G. A., Weber, K. L., & Keiffer, R. F. (2013). The native and introduced fishes of Clear Lake: A review of the past to assist with decisions of the future. *California Fish & Game*, *99*(1), 7–41. Retrieved from https://nrm.dfg.ca.gov/FileHandler.ashx?DocumentID=69445&inline=1

Toffolon, M., Piccolroaz, S., & Calamita, E. (2020). On the use of averaged indicators to assess lakes' thermal response to changes in climatic conditions. *Environmental Research Letters*, *15*(3), 034060. https://doi.org/10.1088/1748-9326/ab763e

Toffolon, M., & Serafini, M. (2013). Effects of artificial hypolimnetic oxygenation in a shallow lake. Part 2: Numerical modeling. *Journal of Environmental Management*, *114*, 530–539. https://doi.org/10.1016/j.jenvman.2012.10.063

Valipour, R., Rao, Y. R., León, L. F., & Depew, D. (2019). Nearshore-offshore exchanges in multi-basin coastal waters: Observations and three-dimensional modeling in Lake Erie. *Journal of Great Lakes Research*, *45*(1), 50–60. https://doi.org/10.1016/j.jglr.2018.10.005

Walker, W. W. (1979). Use of hypolimnetic oxygen depletion rate as a trophic state index for lakes. *Journal of Geophysical Research*, *15*(6), 1463–1470. https://doi.org/10.1029/WR015i006p01463

Welch, E. B., & Cooke, G. D. (1995). Internal phosphorus loading in shallow lakes: Importance and control. *Lake and Reservoir Management*, *11*(3), 273–281. https://doi.org/10.1080/07438149509354208

Wilhelm, S., & Adrian, R. (2008). Impact of summer warming on the thermal characteristics of a polymictic lake and consequences for oxygen, nutrients and phytoplankton. *Freshwater Biology*, *53*(2), 226–237. https://doi.org/10.1111/j.1365-2427.2007.01887.x

Woolway, R. I., & Merchant, C. J. (2019). Worldwide alteration of lake mixing regimes in response to climate change. *Nature Geoscience*, *12*(4), 271–276. https://doi.org/10.1038/s41561-019-0322-x

Yang, P., Xing, Z., Fong, D. A., Monismith, S. G., Tan, K. M., & Lo, E. Y. M. (2015). Observations of vertical eddy diffusivities in a shallow tropical reservoir. *Philosophical Transactions of the Royal Society B*, *9*(3), 441–451. https://doi.org/10.1016/j.jher.2014.09.004

Yvon-Durocher, G., Jones, J. I., Trimmer, M., Woodward, G., & Montoya, J. M. (2010). Warming alters the metabolic balance of ecosystems. *Philosophical Transactions of the Royal Society B: Biological Sciences*, *365*(1549), 2117–2126. https://doi.org/10.1098/rstb.2010.0038